04-25-96 11:25:26 .. 00101

Fate and Transport of Plutonium-239 + 240 and Americium-241 in the Soil of Rocky Flats, Colorado

M. Iggy Litaor,* G. R. Barth, and E. M. Zika

ABSTRACT

Actinides contamination of soils around Rocky Flats, CO, resulted from leaking drums of Pu-contaminated oil stored at an outdoor site. The transport of these actinides through the soil to groundwater was studied using an advanced monitoring system (MS). The fully automated, remotely controlled MS gathered real-time data on soil water content, groundwater level, and timing of gravitationally flowing water. Controlled rain simulations coupled with measurements of volume flux and actinide activities provided essential information about the fate and transport of Pu-239 + 240 and Am-241. Volume fluxes at most sampling locations were similar, regardless of the antecedent moisture or the duration, frequency, and intensity of the simulated rain. Actinide activities were not correlated with the measured volume flux, or the duration, frequency, and intensity of the simulated rain. Flow was facilitated primarily via macropore channeling. The relatively short residence time precluded a continuous interaction between the soil and the flowing water, which minimized the movement of actinides in the soil. Actinide activities in the interstitial water collected from the upper 20 cm of the soil were significantly higher ($P > 0.001$) than water collected at deeper sampling depths (20–70 cm). Actinide activity in water samples from the deepest sampling depth (40–70 cm) did not exceed 0.4 Bq/L. These results suggest that, under the experimental conditions, the movement of actinides was restricted to the top 20 cm. A transport mechanism involving discrete Pu oxide particles, coupled with macropore channeling is proposed to explain the observed actinide activities in the soil.

University of Colorado, Dep. of Civil, Environ., and Architectural Eng., Boulder, CO 80309-0428. Received 7 Aug. 1995. *Corresponding author (litaor@bechtel.colorado.edu).

Published in J. Environ. Qual. 25:•••–••• (1996).

Abbreviations: MS, monitoring system; GPR, ground penetrating radar; TDR, time-domain reflectometry; ZTS, zero-tension samplers; PVC, polyvinylchloride; TS, tension samplers; PTFE, polyethylene tetrafluoride; CSI, Campbell Scientific Inc.; ESP, exchangeable sodium percent.

PLUTONIUM CONTAMINATION OF SOILS at Rocky Flats Environmental Technology Site (the Site), located north of Golden, CO, originated primarily from a former storage site where steel drums were used to store Pu-contaminated industrial oils from 1958 to 1968 (Krey and Hardy, 1970; Seed et al., 1971). Leakage from these drums contaminated surface soils and plants. Plutonium particles entrapped in the fine fraction of the surface soils were subsequently resuspended by winds and deposited across the soilscape east of the Site (Litaor, 1995a,b; Litaor et al., 1995). Weapons-grade Pu processed at the Site was reported to have isotopic composition of: 0.04% Pu-238, 93.3% Pu-239, 6% Pu-240, 0.58% Pu-241, and 0.04% Pu-242 (Krey and Krajewski, 1972; Martell, 1975). The initial Am-241 activity in the weapons-grade Pu processed at the Site did not exceed 10^{-4}% (Krey et al., 1976). Thus, nearly all the Am-241 activity in the soil around the Site resulted from radioactive decay of Pu-241 ($t_{1/2}$ = 14.4 yr) to Am-241.

The fate and transport of actinides in soil, as well as the soil physicochemical properties that govern the behavior of these actinides, are poorly understood. Hakonson et al. (1981) reviewed the transport of Pu in terrestrial systems and asserted that leaching of soluble Pu through the soil is probably an important phenomenon. Other findings support this claim. For example, Onishi et al. (1981) found that adsorbed Pu can be readily moved through the aqueous environment in colloidal forms. More recently, Penrose et al. (1990) found that Pu and Am were transported in groundwater for at least 3.4 km down-gradient from the point of discharge. These actinides were tightly or irreversibly bound to colloidal material (25–450 nm).

Minimal research has been conducted on the fate and transport of actinides in soils of the Site. Krey et al. (1976) speculated that the successful application of the diffusion term in their soil-Pu transport model related to the transport of Pu in soil interstitial water. No data were collected to support this hypothesis, however. More than 90% of the actinide activity in soils at the Site occurs in the upper 12 cm of the soil, regardless of the soil series, or distance and direction from the source of release (Litaor et al., 1994). However, there is strong evidence that small amounts of actinides move to greater depths through a network of macropores formed by decayed root channels and other biological processes (Litaor et al., 1994). For example, groundwater samples collected from a well located 10 m downhill from contaminated soils exhibiting an extensive network of macropores, showed occasionally elevated activities of Pu-239+240 (maximum observed activity of 0.85 Bq/L). This result indicated that under certain conditions, which are currently poorly understood, Pu-239+240 may be transported from the contaminated surface soil to groundwater.

The general goal of this study was to assess the fate and transport of Pu-239+240 and Am-241 in the soil environment. This information is essential for risk assessment and selection of remedial alternatives at the Site. The specific objectives of the study were: (i) to ascertain the mobility of actinides in contaminated soil under simulated conditions of extreme rainfall events, and (ii) to study the edaphic factors that control the movement of Pu-239+240 and Am-241 from the contaminated soil to groundwater.

METHODS

Soil Sampling

Five soil pits along a contaminated toposequence (Fig. 1) were excavated with a backhoe, and sampled for actinide activities and for physical, chemical, and mineralogical properties (see Litaor et al., 1994 for details). Each pit was approximately 5 m long, 1 m wide, and 1 m deep. Before sampling

Best Available Copy

DOCUMENT CLASSIFICATION REVIEW WAIVER PER CLASSIFICATION OFFICE

ADMIN RECORD
SW-A-004642

and insertion of the monitoring system, the entire soil face was thoroughly scraped to eliminate the smearing effect induced by the backhoe. Random sampling within the vadose zone in areas characterized by preferential flow is likely to underestimate contaminant transport (Kung and Donohue, 1991). Hence, the number of pits investigated and their exact positions were determined by a ground penetrating radar (GPR) survey that was used to locate subsurface lateral discontinuities (Litaor et al., 1994). The lateral discontinuities may facilitate increased transport of actinides due to preferential pathway. Pits 2 to 5 were excavated to diagonally intersect the lateral discontinuities as determined by the GPR image. Pit 1 was located approximately 4 m above a spring (locally known as SW-53) that receives most of its water from an aquitard located below the toposequence.

Pit 1 located at the toeslope position (Fig. 1) was approximately 1 m above groundwater and was classified as fine-loamy, mixed (calcareous), mesic Cumulic Haplustoll. Pits 2 to 4 located along a colluvial footslope position exhibited variable depth to groundwater (1.5 to 2.5 m), and were classified as fine-loamy, mixed, mesic Aridic Argiustoll. Pit 5, located at a steep backslope position approximately 6 m above groundwater, was classified as loamy-skeletal, mixed mesic Aridic Argiustoll. The toposequence was characterized as a mesic mixed grassland. The dominant species are common mullein (*Verbascum thapsus* L.), 'Kentucky' bluegrass (*Poa pratensis* L.), Japanese brome (*Bromus japonicus* Thunb. ex Murr.), prickly lettuce (*Lactuca serriola* L.), Canada thistle [*Cirsium arvense* (L.) Scop.], Baltic rush (*Juncus balticus* Willd.), western wheatgrass (*Agropyron smithii* Rydb.), alysuum (*Alyssum minus*), and cheatgrass (*Bromus tectorum* L.). The mean foliar cover was approximately 90% and the ground cover was 80% litter, 19.8% vegetation, and 0.2% rock.

The soil pits were back-filled by hand after the installation of the monitoring system in the upslope face of the pit, to minimize flow interference and convergence into an open pit (Atkinson, 1978). During back-filling, special attention was given to soil placement to prevent flow between the instrumented face and the refilled material. The reconstruction of the pits also paid particular auention to the origin of the spoil material (i.e., the spoil material that originating from the A horizon was placed against the A horizon, etc.).

Hydraulic conductivity was measured in the field using a modified tension infiltrometer (baseplate diam. of 22.6 cm) described by Ankeney et al. (1991). Infiltration experiments were conducted in all the major horizons of the five pits at five near-equally spaced locations along the pit wall across from the installed monitoring system.

Monitoring System

The monitoring system (MS) consisted of five major modules: (i) automated zero-tension samplers that collected water flowing gravitationally, mainly through macropores; (ii) tension samplers (also known as tension lysimeters) that collected interstitial water at matric potential >-5 kPa; (iii) time-domain reflectometry (TDR) probes, which measured in-situ water content; (iv) five piezometers that monitored groundwater level; and (v) a telemetry communication network coupled with a graphic user interface that processed and archived remotely acquired data.

Zero-Tension Samplers

Zero-tension samplers (ZTS) were troughs designed to collect gravitationally flowing water (Litaor, 1988). A ZTS consisted of a half-section polyvinylchloride (PVC) pipe (36 cm by 15 cm) capped at one end. Significant higher activity of Pu-239+240 was observed in soils with abundant macropores in Pits 3 and 4 compared with the surroundings soil matrix (Litaor et al., 1994). Hence, the ZTS were inserted into the soil face using hydraulic jack in locations where macropores (>1 mm) were evident. This intrusive installation occasionally created or enhanced existing macropores, which in turn increased the volume flux and potentially the actinides flux. This apparent bias agrees well with the underlying purpose of this investigation, namely the fate and transport of Pu-239+240 and Am-241 under extreme conditions. It was also assumed that with time (~12 mo, see Litaor, 1988) the disturbed soil would reach a steady state and past intrusive activity would exert little influence on flow characteristics. The volume flux as defined here is the water volume collected by the ZTS divided by the ZTS area (0.054 m^2).

In general, five ZTS were installed within a specified soil depth increment for a total of 15 ZTS per pit (Fig. 2). The sampling depth increments were (in cm): 0 to 20, 20 to 40, and 40 to 70. The exact number of ZTS was determined from visual examination of the location and distribution of macropores, and field assessment of the vertical and lateral heterogeneity of the soil. It was assumed that the gravitationally flowing water collected by the ZTS represented primarily macropore channeling, with limited additional flow from the soil matrix (Luxmoore, 1991).

The gravitationally flowing water intercepted by each ZTS was collected in a 500-mL bottle located on a load cell in one of three enclosures in the bottom of each pit (Fig. 2). In general, five collection bottles were placed on each load cell for a total of 15 collection bottles per pit. Load cells continuously monitored, by weight, the timing of the flow. As water accumulated in the bottles, the load cell measured the corresponding change in mass up to 3.4 kg. Each load cell was connected through a multiplexer to a data-logger that continuously monitored the total amount of water collected from each sampling depth. Samples were collected from the underground bottles using a vacuum-pump collection manifold.

Tension Samplers

In each pit, 18 tension samplers (TS) extracted interstitial water flowing at matric potentials <-5 kPa. The TS consisted of hollow, porous cylinders (5-um and 10-um pore size) made of polyethylene tetrafluoride (PTFE) (Prenart Equipment ApS, Denmark) connected to a vacuum system. We selected to use the chemically inert PTFE sampler to reduce the sorption capacity exhibited by the more commonly used ceramic porous cup sampler (Litaor, 1988). All the PTFE samplers were treated with silica flour before installation to reduce their inherit hydrophobicity.

The TS were inserted into the pit wall in locations where visible macropores were absent. To insert the TS, a soil core was extracted from the pit face and mixed with distilled water to make a slurry. The slurry and the TS were placed back into the core hole. The TS was pushed into the pit face until it was entirely submerged by the slurry, ensuring a full contact between the slurry and the surrounding soil. Since no sieving of the soil core was conducted, the texture of the slurry and the surrounding soil remained approximately the same, preventing the formation of a major textural break that may affect the flow characteristics of the soil around the TS. The TS were grouped with TDR probes in six clusters per pit, with three tension samplers in each cluster (Fig. 2). Two clusters were located in each of the three soil-depth intervals described above.

The automated TS collection system at each pit consisted

of: (i) a vacuum-pump enclosure containing a pump, 12-V deep-cycle battery, solenoid valves, and controls; (ii) an insulated box containing six 1000-mL sample-collection vessels; and (iii) three 18-W solar panels used to recharge the 12-V battery. Each vessel collected water drawn from a separate cluster. When soil water content measured by the TDR probes decreased below pre-set drying conditions, the corresponding TS clusters were activated for 15-min periods at least nine times per day at −30 kPa pressure. The vacuum generated inside the TS extracted the soil interstitial water from the soil matrix into the TS. The limiting factor in applying the vacuum inside the TS was the daily solar condition, which determined the rate of battery recharge.

Time-Domain Reflectometry Probes

Soil water content was monitored by TDR probes. The TDR system manufactured by Campbell Scientific Inc. (CSI) was used. A single probe system consisted of two wave guides connected to parallel transmission cable lines. The probes were linked to a cable tester (Tektronix 1502B) through a hierarchy of multiplexers. Three tiers of multiplexers were necessary to monitor all the TDR probes. At sampling time, the datalogger activated the appropriate multiplexers, triggered the cable tester, analyzed the cable tester signal, and advanced the multiplexer, repeating the process until 120 TDR probes had been sampled. A balance transformer was used to match the impedance of the parallel transmission cables to the 50-ohm coaxial cable that connected the cable tester with the multiplexers. The CSI datalogger utilized Ledieu's et al. (1986) algorithm to convert the transit time of the electro-magnetic pulse along a probe into volumetric soil moisture content.

In each pit, probes were inserted in clusters of four, with two clusters per depth at three different depths for a total of 24 probes per pit (Fig. 2). Each set of four probes was clustered with three tension samplers. The parallel waveguides were placed horizontally into a soil horizon. The number of TDR probes used in this study was determined from field observations of lateral and vertical heterogeneity of the soils.

Rain Simulation

An automated rain simulator, which consisted of a delivery and an application system, was used to conduct rainfall simulation experiments over the five test pits during the summer of 1993. The delivery system included a 9.14-m head sump pump (Teal 4.5 Amp/110 V) that was used to prime a centrifugal pump (91.5 L/min, Black & Decker 5 Amp/110 V) with tap water obtained from a 1135-L reservoir. The exchangeable sodium percent (ESP) in all the soil pits was <0.4, and so any differences in ionic strength between the tap water and rain water had no significant impact on the erodibility and leachability of the soil (e.g., Shainberg et al., 1994). The centrifugal pump supplied the tap water to the spray header at a constant rate and pressure. A pressure regulator (0–1724 kPa, Spraying System Model No. 11438-250) was used to maintain the required pressure while a flow sensor (Omega FB603) and flow monitor (Omega DPF402) monitored the rate of application. The application system consisted of an automated spray platform, a 122-cm spray header that held three equally spaced Unijet flat spray nozzles. The tips of the nozzles were interchangeable to allow application rates varying from 5.87 to 9.54 L/min. The application system traveled on an aluminum frame (6.09 m in length) that extended beyond the ends of the pit to eliminate boundary effects. The frame dimensions also provided room for the placement of three rain gauges underneath the simulator, beyond the area of the instrument pit to verify the uniformity of the rain application. Uniformity of the spray application was aided by a wind skirt that reduced the deformation of the spray pattern by wind.

Twenty-three rain-simulation experiments were performed between Julian Day 179, 1993 and Julian Day 211 in 1993. Simulation variables included duration, intensity, and frequency (Table 1). The rain simulator was designed to simulate rainfall events of 10-, 25-, 50-, and 100-yr return periods. A return period is defined as the average recurrence interval between events equaling or exceeding a specified magnitude. Events with these return periods were selected to provide a range of rain events that might produce flow of water through the soil. The intensities and duration of 10-, 25-, 50-, and 100-yr return events were calculated using guidelines and historical data of the Golden area, from The Precipitation-Frequency Atlas of the Western United States (U.S. Weather Bureau, 1961).

The vegetation in all pits was clipped to 5 to 10 cm above the ground surface to ensure that the water reached the soil surface and to compensate for the smaller size and terminal velocities of the simulated rain drops. After each rain simulation, the pits were covered with thick plastic sheeting to increase infiltration by reducing evaporation. These measures were also taken to simulate worst-case scenarios of Pu-239+240 and Am-241 transport from the soil to groundwater.

Laboratory Analysis

The volume of soil interstitial water, collected from each ZTS or TS, was measured to the nearest 1 mL using a graduated cylinder and briefly described for sample appearance (i.e., color, clarity, sediment content, and biota—i.e., earthworms). Specific conductance, temperature, pH, and alkalinity of the water were also measured in the field. The Pu-239+240 and Am-241 activities in unfiltered samples of the soil interstitial water were measured by alpha spectrometry in a commercial laboratory. The soil interstitial water were digested using a microwave dissolution procedure and the Pu oxidation state was adjusted with $NaNO_2$. The solution was then passed through an anion exchange column to separate the Pu from the solution (Talvitie, 1971). The Pu was eluted from the column with HCl–NH_4I solution, was acidified with HNO_3, and the sample was heated to dryness. The sample was redissolved and electroplated onto stainless steel discs. Upon completion of the electroplating, NH_4OH was added to the solution to prevent redissolution of the deposit.

To isolate the Am-241 from the soil interstitial water the sample was leached with HNO_3. Hydroxides and carbonate-forming elements (e.g., Am) were precipitated out of the leachate with NH_4OH and $(NH_4)_2CO_3$, respectively. After drying, the precipitate was redissolved with nitric acid and passed through an anion-exchange column to remove the nontrivalent actinides. Trivalent actinides and lanthanides were coprecipitated with Ca using oxalic acid, Ca carrier, and NH_4OH. The precipitate was redissolved with HCl and passed through a column of mixed anion–cation resin to remove some of the Ca and all of the Fe. Cesium and the remainder of the Ca were extracted from the solution using double extraction into dibutyl-*N*,*N*-diethycarbamylphosphonate, a back extraction into dilute HNO_3, and then heating to dryness. The sample was redissolved in a dilute acid solution and passed through an anion-exchange column to remove trivalent lanthanides. This column was washed with mixture of alcohol, dilute acids, and NH_4SCN for partial separation of Am from Cm. The sample was then converted to a sulfate form and heated to dryness. Following this, the sample was redissolved and electroplated onto stainless-steel discs. Upon completion of the

electroplating, NH_4OH was added to the solution to prevent redissolution of the deposit.

Data Quality

An extremely rigorous quality assurance and quality control protocols were established to meet all the requirements of a waste site characterization study. These practices were approved by the regulatory agencies and were enforced by an independent party. A detailed account of the quality assurance and quality control practices, the results of field and laboratory duplicates, counting errors, data qualifiers, below detection levels, and other pertain QA information is given in EG&G (1995).

Statistical Analysis

Comparisons of actinide activities and ratio, chemical concentrations, volume flux, and soil moisture following the various rain simulation conditions (i.e., recurrence and intensity) were conducted using nonparameteric techniques (Norusis, 1994). Multiple comparisons among actinide activities and ratio, volume flux, and soil moisture at three sampling intervals were performed using the Kruskal-Wallis test. A comparison of the chemistry of the soil interstitial water collected by the ZTS and TS in the A horizon was performed using the Wilcoxon Rank Sum Test. The Wilcoxon Rank Sum and the mean rank of the Kruskal-Wallis Test provided a measure of similarity between the data sets, where the smallest datum was assigned the Rank 1 and the largest datum in a data set was assigned the Rank m before the appropriate statistic was computed (see Gilbert et al., 1987, p. 248–252).

RESULTS AND DISCUSSION

Activity of Actinides in Soil

Approximately 90% of the Pu-239+240 and Am-241 activity in the soils under study was observed in the upper 12 cm, below which a rapid decrease of actinide activity occurred (Fig. 3). However, appreciable Pu-239+240 activities were observed at depths of 24 and 36 cm in Pit 5 (1032 and 895 Bq/kg, respectively), and increases in Pu and Am activities were also observed at 48 and 96 cm in Pit 4 (Fig. 3). These actinide activites are significantly higher than previously reported for soils at the Site. For example, Little and Whicker (1978) reported a mean activity of 473 Bq/kg for Pu-239+240 at a sampling depth of 18 to 21 cm in a study area known as *macro plot 1*, located 100 m southwest of Pit 5. This apparent discrepancy can be explained by the edaphic factors obseved in the study area. Pit 5 is located on a steep slope (12%) and its upper 48 cm exhibited a very coarse texture (Table 2). Pits 1 through 5 exhibited high hydraulic conductivities in the A horizon, and occasionally, in the B horizons (Table 2). These factors probably facilitated the translocation of actinides to greater depths than previously reported.

Activity of Actinides in Soil Interstitial Water

Plutonium-239+240 and Am-241 activities in the soil interstitial water collected by the ZTS showed a clear distribution with depth (Fig. 4). Actinide activities were significantly higher in the upper 20 cm than in the deeper sampling depths (Table 3). This pattern was consistent in all rain simulations. The highest Pu-239+240 and Am-241 activities observed in the deepest sampling layer did not exceed 0.4 Bq/L, even under the most extreme rain-simulation conditions. The activity of Pu-239+240 in the soil interstitial water at most sampling locations and rain simulations was higher than that of Am-241. Their relative distribution with depth was remarkably similar, however (Fig. 4), and Am-241/Pu-239+240 ratios did not increase significantly with depth (Table 4). These ratios agreed reasonably well with the activity ratio calculated (0.17) and measured (0.19) in soils of the Site (Litaor, 1995a). The results indicated that Am-241 does not move faster than Pu-239+240 in the soils of the Site. These findings are in disagreement with the notion advanced by Fowler and Essington (1974), who ascertained that Am-241 is more soluble than Pu-239+240 and may become the radionuclide of prime concern because of a faster migration rate in soils.

In general, the distribution of actinide activities in the soil interstitial water suggested that the movement of Pu-239+240 and Am-241 was limited to the upper 20 cm of the soil, with little transport of actinides to the deeper horizons. However, a considerable number of outliers and extreme activities were observed in the top soil sampling layer, and some in the second sampling layer, especially after the 100-yr event (Fig. 4). The existence of these outliers and extreme activities in the soil interstitial water indicated that under the experimental conditions there is a potential for translocation of actinides from the contaminated top horizon to deeper horizons of the soil, and possibly to groundwater.

Flow Characteristics during Rain Simulations

To examine the hydrological conditions that produced the observed actinide distributions discussed above a detailed analysis of the gravitational water flow and the antecedent soil moisture conditions was performed. In general, the volume flux of the soil interstitial water collected by the ZTS was of comparable magnitude, regardless of sampling depth (Table 5). The volume flux was defined as the water volume collected by the ZTS, divided by the ZTS area (0.054 m^2) per rain simulation. The relatively uniform distribution of the volume flux with depth was in apparent disagreement with the saturated hydraulic conductivity (K_s) distribution in the soil (Table 2). The average K_s decreased from 14.3 cm/h in the A horizon to 2.5 cm/h in the B horizon. This decrease corresponded well with the increase in clay content and abundance of expandable clay minerals with depth (Table 2). However, the K_s values exhibited a significant number of outliers in all measured locations because of extensive macropore networks in the soils. These macropores originated from earthworm activity and decayed root channels (Litaor et al., 1994). As described above, the ZTS were installed in locations where macropores were clearly visible in the field. Thus, the vertical distribution of the volume flux indicated that macropore channeling was an important flow attribute in the soil and that most of the macropores observed in the field and sampled with the

ZTS were hydrologically active to at least 70 cm below the surface.

The gravitationally flowing water was characterized by short residence time in the soil. A plot of the load-cell output versus time, measured in Pit 3 during three successive rain simulations, showed that the flow in the first and third sampling depth intervals (10–20 cm and 40–70 cm, respectively) occurred mostly as brief pulses of short duration of <2 h (Fig. 5). The abrupt end of flow, as recorded by the load-cell output, is characteristic of macropore channeling. This abrupt end of flow was typical of most locations, under all rain simulation conditions. The second sampling interval (20–40 cm) exhibited an initial pulse that lasted for 2 h, followed by a steady increase in load cell output. Although the ZTS were designed to collect gravitationally flowing water mainly through macropores, undoubtedly some flow originated from the meso-micro pores domain (i.e., pores <0.1 cm in diam.). The distribution of the meso-micro pores in the soil is unknown, but the observed load-cell pattern suggested that some flow in the second sampling interval was generated from this domain and lasted for more than 10 h.

The relationships between volume flux and antecedent soil moisture were examined by comparing their vertical distribution in the soil after each rain simulation. In general, the antecedent soil moisture showed a consistent pattern with depth (Fig. 6). The top sampling interval was always drier than the deeper sampling intervals under all simulated rain conditions. The rapid drying observed in the top sampling layer strongly suggests considerable evapotranspiration from the A horizon. The increased soil moisture content with depth can be explained by the increased clay content in the subsurface horizons (Table 2). Higher clay content facilitated higher water-holding capacity, as well as the influence of the capillary fringe in the deepest horizons, which are 30 to 40 cm above the water table.

The antecedent soil moisture profile during the first four rain simulations provided insight into the conditions in which macropore channeling can be activated. During the first two rain simulations of 10-yr recurrence with an intensity of 0.79 mm/min, the top horizon did not reach saturation, and the wetting front did not advance beyond 20 cm following the first simulation and 40 cm following the second simulation (Fig. 6). The top sampling interval finally reached saturation following the third rain simulation of 25-yr recurrence with an intensity of 0.99 mm/min; however, the wetting front did not reach the deepest sampling interval. Following the 4th rain simulation of 50-yr recurrence with an intensity of 1.14 mm/min, the entire soil profile reached saturation (Fig. 6). Gravitationally flowing water was collected throughout the rain simulation sequence, regardless of the antecedent soil moisture conditions. There was no statistical difference in volume measured at the three sampling intervals during the unsaturated and the saturated conditions. These results strongly indicated that macropore channeling occurred under both unsaturated and saturated conditions.

The effect of antecedent soil moisture on the magnitude of volume flux was further assessed by comparing the volume collected after similar rain events of different intensity and antecedent soil moisture conditions recorded 30 min before the rain simulations (Table 6). The volume flux was significantly higher during the 100-yr event of 2.03 mm/min intensity than the volume flux collected during a longer duration, lower intensity rain simulation of the same return period. The higher intensity combined with wetter antecedent soil moisture in Pit 2 produced the intuitively expected results. However, these expected relationships were not observed during subsequent rain simulations of various magnitude and intensities (Table 6). The inconclusive association between antecedent soil moisture and volume flux obtained in this study have been reported elsewhere. For example, Quisenberry and Phillips (1976) found deeper movement of water and Cl when the antecedent soil moisture was high, whereas White et al. (1986) found the opposite relationships. In the latter study—of undisturbed cores of a structured clay soil—the water infiltrating dry soil bypassed most antecedent soil moisture, whereas in wetter soil, the hydrologically active macropores may have been more constricted, resulting in reducing pore water velocity.

Transport Mechanisms of Actinides

The actinide activities in the soil interstitial water were completely uncorrelated with the magnitude of volume flux (r^2 = 0.006). This profound lack of correlation was consistent under all rain simulations. Furthermore, Pu-239+240 activity in the soil interstitial water exhibited no relationship with the magnitude or intensity of the simulated rain, nor the antecedent soil moisture (Table 6). This pattern probably can be explained by the transport processes that govern the distribution of Pu-239+240 and Am-241 in the soil and the physicochemical characteristics of these radionuclides in the soil. Most Pu-239+240 exists in the soil as discrete particles associated with host soil grains. The term *discrete particle* is defined here as an agglomerated particle containing a large number of host soil grains and Pu oxides. The host soil grains in these soils consisted of organic matter (45–65%), sesquioxides (20–40%), and intractable residue (10–15%) (Litaor and Ibrahim, 1996). Several studies have documented the nature and extent of the discrete particle phenomenon in the soils of Rocky Flats. For example, McDowell and Whicker (1978) studied soil collected from Macro Plot 1, located 100 m southwest from Pit 5 and isolated a PuO_2 particle of 6.86 μm diameter. This particle was identified as an agglomerate of smaller, probably submicron, particles containing as much as 40% by weight Pu in a noncrystalline or organic substance. The measured activity of this particle was 3922 Bq/kg, which accounted for 7% of the activity in that soil sample. Large variability was observed in the particle-size distribution of Pu oxides in this soil sample, suggesting that an unspecified mechanism may exist that either concentrated Pu particles in the soil, or caused a breakdown of Pu particles into smaller adjacent particles (McDowell and Whicker, 1978). Hayden (1975) showed

that the number of discrete Pu particles measured in-situ on the soil surface located 1 km from the source varied between 0 to 29 particles along a 3-m sampling interval, with a dominant Pu oxides particle diameter of 0.5 μm that could be traced to the former storage site. Hayden (1975) indicated that much larger Pu oxide particles were observed near the source (2–3 μm).

Movement of the discrete particles of Pu oxides within the soil probably results from the force exerted by the gravitationally flowing water on the macropore wall. Occasionally, dislodgement of a larger discrete particle from the macropore wall could result in higher activity of Pu-239+240 or Am-241 in the soil interstitial waters. The timing and location of the dislodging of the discrete particles is difficult to predict. For example, the highest activity of Pu-239+240 in soil interstitial water collected from the top horizon was observed following a 25-yr event, rather than larger and more intense rain simulations (see Fig. 4).

On the basis of the vertical distribution of volume flux, actinide activity and the various edaphic conditions discussed above, we hypothesize that the translocation of actinides to deeper soil horizons may be constrained by macropores too small to accommodate the transport of the discrete particles. The observed short duration of macropore flow, which indicates that there is no continous interaction between the soil and the flowing water, and the presumed small soil volume in which macropore flow occurs, further minimizes the movement of Pu oxide particles in the soil. These hydrological constraints can account for the lack of observed correlation between Pu-239+240 and Am-241 activities in the interstitial water, volume flux, and other rain simulation parameters (e.g., intensity).

Pu-239 + 240 Activity and Solute Concentrations in Soil Solution at Matric Potential < -5 kPa

During periods of significant evapotranspiration between rain simulations (see Fig. 6), the soil water content measured by the TDR probes decreased below preset drying conditions, and the corresponding TS clusters were activated. Although the TS were activated for most of the drying periods depicted in Fig. 6, only a limited amount of water was extracted at a matric potential < -5 kPa. The limited amount of water extracted by the TS probably resulted from the abundance of clay content (principally smectite) in the soil matrix, especially in deeper horizons (Table 2).

Activities of Pu-239+240 and Am-241 were significantly higher in samples collected by ZTS than in samples collected at greater matric potential (Table 7). This pattern most likely resulted from translocation of discrete Pu oxide particles via macropore channeling. The water collected by the TS was mainly extracted from the soil matrix, which seems to limit the movement of Pu oxides. Conversely, specific conductance, alkalinity, and pH of the samples collected at matric potentials < -5 kPa (drier conditions) were significantly higher than samples collected via macropore channeling (Table 7). Taken together, these findings suggest that the water collected at higher matric potentials exhibits longer residence time, which in turn allows prolonged interaction with the soil matrix and results in higher concentrations of electrolytes. The higher pH and alkalinity observed in water samples collected at greater matric potential was comparable with the soil pH and alkalinity (see Table 2), indicating near-equilibrium conditions for these interstitial water.

Concluding Remarks

This study has provided empirical information regarding the fate and transport of actinides in the soils of Rocky Flats. Under the experimental conditions, the movement of Pu-239+240 and Am-241 was restricted to the top 20 cm of the soil. The results provide important information required for selecting remedial actions and corrective measures for cleanup. This study has also demonstrated that our current understanding of the edaphic factors that control the fate and transport of actinides in the soil environs is limited.

ACKNOWLEDGMENTS

The authors thank Dr. Larry Woods, Dr. Mary Siders, and Mr. L. Allen for their useful comments on an earlier version of this article. We also thank three anonymous reviewers for their excellent comments.

REFERENCES

Ankeney, M.A., M. Ahmed, T.C. Kaspar, and R. Horton. 1991. Simple field methods for determing unsaturated hydraulic conductivity. Soil Sci. Soc. Am. J. 55:167–170.

Atkinson, T.C. 1978. Techniques for measuring subsurface flow on hillslopes. p. 73–120. *In* M.J. Kirkby (ed.) Hillslope hydrology. John Wiley & Sons, New York.

EG&G. 1995. Draft final. Phase II RFI/RI Report: 903 Pad, Mound, and East Trenches Area, Operable Unit 2. RF/ER-95-0079.UN. U.S. Dep. of Energy, Rocky Flats Environ. Technol. Site, Golden, CO.

Fowler, E.B., and E.H. Essington. 1974. Soils element activities October, 1972–September, 1973. p. 7–16. *In* P.B. Dunnaway and M.G. White (ed.) The dynamics of plutonium in desert environments. NVO-142. Nevada Applied Ecology Group, U.S. Dep. of Energy, Las Vegas, NV.

Gilbert, R.O. 1987. Statistical methods for environmental pollution monitoring. Van Nostrand Reinhold, New York, NY.

Hakonson, T.E., R.J. Watters, and W.C. Hanson. 1981. The transport of plutonium in terrestrialecosystems. Health Phys. 40:63–69.

Hayden, J.A. 1975. Particle size distribution of plutonium on soil surface in Rocky Flats east buffer zone. Second draft, 26 Sept. 1975. Rockwell International, Rocky Flats Plant, Golden CO.

Krey, P.W., and E.P. Hardy. 1970. Plutonium in soil around the Rocky Flats Plant. HASL-235. U.S. Atomic Energy Commission, Health and Safety Lab., New York.

Krey, P.W., E.P. Hardy, and L.E. Toonkel. 1976. The distribution of plutonium and americium with depth in soils at Rocky Flats. HASL-318. U.S. Atomic Energy Commission, Health and Safety Lab., New York.

Krey, P.W., and B.T. Krajewski. 1972. Plutonium isotopic ratios at Rocky Flats. HASL-249. U.S. Atomic Energy Commission, Health and Safety Lab., New York.

Kung, K-J.S., and S.V. Donohue. 1991. Improved solute-sampling protocol in a sandy vadose zone using ground-penetrating radar. Soil Sci. Soc. Am. J. 55:1543–1545.

Ledieu, J., P. Ridder, P. Clerck, and S. Sautrebande. 1986. A method of measuring soil moisture by time-domain reflectometry. J. Hydrol. 88:319–328.

Litaor, M.I. 1988. Review of soil solution samplers. Water Resour. Res. 24:727–733.
Litaor, M.I. 1995a. Uranium isotopes distribution in soils at the Rocky Flats Plant, Colorado. J. Environ. Qual. 24:314–323.
Litaor, M.I. 1995b. Spatial analysis of Pu-239+240 and Am-241 in soil around Rocky Flats, Colorado Plant. J. Environ. Qual. 24: 506–516.
Litaor, M.I., D. Ellerbroek, L. Allen, and E. Dovala. 1995. A comprehensive appraisal of plutonium-239+240 in soils of Colorado. Health Phys. 69:923–935.
Litaor, M.I., and S. Ibrahim. 1996. Plutonium association with selected solid phases in soils of Rocky Flats, Colorado using sequential extraction technique. J. Environ. Qual. 25:(in review).
Litaor, M.I., M.L. Thompson, G.R. Barth, and P.C. Molzer. 1994. Plutonium-239+240 and americium-241 in soils east of Rocky Flats, Colorado. J. Environ. Qual. 23:1231–1239.
Little, C.A., and F.W. Whicker. 1978. Plutonium distribution in Rocky Flats soil. Health Phys. 34:451–457.
Luxmoore, R.J. 1991. On preferential flow and its measurement. p. 12–22. *In* T.J. Gish and A. Shirmohammadi (ed.) Preferential flow. Proc. of the National Symp., Chicago, IL. 16–17 Dec. 1991. Am. Soc. of Agroc. Eng., Chigaco, IL.
Martell, E.G. 1975. Actinides in the environment and their uptake by man. NCAR-TN/STR-110. National Center for Atmospheric Res., Boulder, CO.
McDowell, L.M., and F.W. Whicker. 1978. Size characteristics of plutonium particles in Rocky Flats soil. Health Phys. 35:293–299.
Norusis, M.J. 1994. SPSS for Windows, Release 6.0. SPSS, Chicago, IL.
Onishi, Y., R.J. Serne, E.M. Arnold, C.E. Cowan, and F.L. Thompson. 1981. Critical review: Radionuclide transport, sediment transport, and water quality mathematical modeling; and radionuclide adsorption/desorption mechanisms. Pacific Northwest Lab./ USNRC. NUREG/CR-1322, PNL-2901. Pacific Northwest Lab., Richland, WA.
Penrose, W.R., W.L. Polzer, E.H. Essington, D.N. Nelson, and K.A. Orlandini. 1990. Mobility of plutonium and americium through shallow aquifer in a semiarid region. Environ. Sci. Technol. 24:228–234.
Quisenberry, V.L., and R.E. Phillips. 1976. Percolation of surface applied water in the field. Soil Sci. Soc. Am. J. 40:484–489.
Seed, J.R., K.W. Calkins, C.T. Illsley, F.J. Miner, and J.B. Owen. 1971. Committee evaluation of Pu levels in soils within and surrounding USAEC installation at Rocky Flats, Colorado. DOW Chemical Company, RFP-INV-1. DOW Chemical Co., Golden, CO.
Shainberg, I., J.M. Laflen, J.M. Bradford, and L.D. Norton. 1994. Hydraulic flow and water quality characteristics in rill erosion. Soil Sci. Soc. Am. J. 58:1007–1016.
Talvitie, N.A. 1971. Radiochemical determination of plutonium in environmental and biological samples by ion exchange. Anal. Chem. 43:1827–1830.
U.S. Weather Bureau. 1961. Rainfall frequency atlas of the United States for durations from 30 minutes to 24 hours and return periods from 1 to 100 years. May 1961. Weather Bureau Tech. Pap. 40. U.S. Weather Bureau, Washington DC.
White, R.E., J.S. Dyson, Z. Gerstl, and B. Yaron. 1986. Leaching of herbicides through undisturbed cores of a saturated clay soil. Soil Sci. Soc. Am. J. 50:277–282.

Ed: ?

7

0610152301 litaor
SOIL SCIENCE – J. ENVIRON. QUAL., VOL. 25, JULY-AUGUST 1996
Miles 33 – rm
04-22-96 02:36:14

Table 1. The sequence of rain simulations in the study area.

Julian Day (frequency)	Pit	Recurrence	Intensity
		yr/min	mm/m
179	3	10/60	0.79
180	3	10/60	0.79
182	3	25/60	0.99
183	3	50/60	1.14
187	3	100/60	1.28
188	4	10/60	0.79
189	4	25/60	0.99
190	4	50/60	1.14
193	4	100/60	1.28
194	4	50/60	1.14
194	2	100/60	1.28
195	2	50/60	1.14
196	2	25/60	0.99
197	2	50/30	1.79
200	2	100/30	2.03
200	3	100/30	2.03
201	3	100/60	1.28
202	4	100/60	1.28
203	4	100/60	1.28
204	5	50/60	1.14
207	5	100/60	1.28
208	5	100/120	0.64
209	1	50/60	1.14
210	1	100/60	1.28

0610152302 litaor
SOIL SCIENCE – J. ENVIRON. QUAL., VOL. 25, JULY-AUGUST 1996
Miles 33 – rm
04-25-96 13:45:19

Table 2. Major physical and mineralogical properties of the five soils under study.

Horizon	Depth	Sand	Silt	Clay	>2 mm	$CaCO_3$	pH	Smectite content†	Hydraulic conductivity, K_s				
									X	SD	Min	Max	N
	cm	%				g/kg		%	cm/h				
Pit 1													
A	0–16	46.9	19	34.1	<5	20	7.4	5–30	14.97	5.56	6.77	19.26	4
AB	16–27	27.5	31.8	40.7	<5	56	7.7	30–60			nd		
Bk1	27–58	35.3	29.4	35.3	10	122	8.0	30–60	3.69	3.49	0.74	8.64	4
Bkg	58–76	35.6	31.3	33.1	20	107	7.9	30–60			nd		
Bg	76–103	41.3	29.5	29.2	30	90	7.9	>60	3.41	0.94	2.87	4.50	3
2BCg	103+	34.2	34.1	31.7	50+	56	8.0	>60			nd		
Pit 2													
A	0–7	64.4	19.1	16.5	5	4	7.2	5–30	9.86	3.83	4.53	13.86	5
Bw	7–19	69.8	15.3	14.9	35	3	7.0	5–30			5.23	9.85	2
Bt	19–50	49.1	16.7	34.2	<5	2	7.0	30–60	2.4	1.54	0.69	15.4	3
2Bt	50–105	36.1	27.4	36.5	<5	5	7.0	30–60			nd		
3BCgk1	105+	14.1	40.9	45	<5	27	7.5	>60	2.89	1.91	0.76	4.86	5
Pit 3													
A	0–18	67.3	17.1	15.6	10	10	7.0	5–30	19.2	3.31	13.6	22.27	5
AB	18–35	58.1	15.6	26.3	20	4	7.1	30–60	7.07				1
Bw	35–51	60.4	13.9	25.7	5	2	7.0	30–60	9.33	3.07	4.8	13.32	5
BC	51–120	16.0	44.1	39.9	5	1	7.7	>60	0.34				1
BCk1	120+	22.4	43.6	34.0	<5	35	7.8	>60	0.18				1
Pit 4													
A	0–18	64.1	18.6	17.3	10	6	6.7	5–30	13.9	6.06	9.82	24.55	5
Bt1	18–41	38.4	21.6	40.0	20	4	6.5	5–30	8.7	3.3	4.72	14.0	4
Bt2	41–77	37.9	23.6	38.5	25	1	7.5	30–60	2.9	3.3	0.69	6.67	3
BCg	77–108	38.6	23.9	37.5	<5	9	7.3	>60			nd		
2BCg	108+	24.4	37.2	38.4	<5	4	7.8	>60			nd		
Pit 5													
A	0–15	62.3	22.3	15.4	30	9	7.6	5–30	13.6	6.0	7.24	21.19	5
Bt	15–48	57.7	20.5	21.8	80	9	7.6	5–30	6.7	3.8	2.54	10.51	4
Btg	48–120	43.8	25.9	30.3	5	6	6.0	>60	3.0				1

† Relative abundance of clay-size (< 2 μm).

Table 3. Comparison between Pu-239 + 240 activity in soil solutions collected by the ZTS at three sampling depths across the toposequence following the succession of rain simulations as outlined in Table 1. Am-241 activity in soil solutions exhibited similar pattern (not shown).†

Rain simulation	Depth	Pu-239 (Bq/L) X	m	SD	N	Mean rank	Kruskal-Wallis test
10 yr	0–20	0.71	0.42	0.62	8	12.8	$\chi^2 = 7.1$; $P > \chi^2 = 0.03$
	20–40	0.78	0.28	1.01	9	11.1	
	40–70	0.07	0.05	0.04	3	2.3	
25 yr	0–20	2.57	0.86	4.8	9	17.4	$\chi^2 = 11.3$; $P > \chi^2 = 0.003$
	20–40	0.3	0.23	0.15	7	13.5	
	40–70	0.08	0.06	0.06	8	6.0	
50 yr	0–20	1.5	0.46	2.8	33	49.4	$\chi^2 = 15.6$; $P > \chi^2 = 0.0004$
	20–40	0.19	0.18	0.14	26	33.3	
	40–70	0.13	0.08	0.1	17	25.2	
100 yr	0–20	1.5	0.64	1.9	53	83.6	$\chi^2 = 38.9$; $P > \chi^2 = 0.0001$
	20–40	0.28	0.19	0.33	41	49.8	
	40–70	0.16	0.15	0.09	28	36.6	

† X represents arithmetic mean, m is the median, SD is the standard deviation, and *N* represents the number of measurements.

0610152304 litaor
SOIL SCIENCE – J. ENVIRON. QUAL., VOL. 25, JULY–AUGUST 1996

Table 4. Am-241/Pu-239 + 240 ratios in soil interstitial water collected by the ZTS across the toposequence at three depths followed all rain simulations.†

Depth	Am-241/Pu-239 + 240 X	m	SD	N	Mean rank
cm					
0–20	0.24	0.16	0.48	103	132
20–40	0.16	0.15	0.10	83	110
40–70	0.16	0.15	0.08	56	116
Kruskal-Wallis Test; $\chi^2 = 4.98$; Prob > $\chi^2 = 0.08$					

† X represents arithmetic mean, m is the median, SD is the standard deviation, and *N* represents the number of measurements.

Table 5. Comparison between volume flux collected by the ZTS at three sampling depths across the toposequence following the succession of rain simulations as outlined in Table 1.†

Rain simulation	Depth	N	Flux (cm/event) X	m	SD	Mean rank	Kruskal-Wallis test
	cm						
10 yr	0–20	8	0.43	0.35	0.26	11.8	$\chi^2 = 1.5$; $P > \chi^2 = 0.45$
	20–40	9	0.38	0.37	0.27	10.5	
	40–70	3	0.23	0.22	0.04	6.83	
25 yr	0–20	9	0.58	0.40	0.37	12.2	$\chi^2 = 0.02$; $P > \chi^2 = 0.98$
	20–40	7	0.53	0.50	0.15	12.6	
	40–70	8	0.59	0.52	0.32	12.6	
50 yr	0–20	33	0.64	0.70	0.34	44.8	$\chi^2 = 4.97$; $P > \chi^2 = 0.08$
	20–40	26	0.44	0.38	0.31	32.6	
	40–70	17	0.50	0.48	0.32	35.1	
100 yr	0–20	53	0.62	0.49	0.36	63.9	$\chi^2 = 0.77$; $P > \chi^2 = 0.67$
	20–40	41	0.55	0.49	0.26	61.5	
	40–70	28	0.55	0.44	0.38	56.7	

† X represents arithmetic mean, m is the median, SD is the standard deviation, and N represents the number of measurements.

Table 6. The relationships between volume flux collected immediately after rain simulations, antecedent soil moisture conditions measured before rain simulations of similar magnitude but of different intensity and Pu-239 + 240 activity in the soil interstitial water after these simulations.

Pit and rain simulation	Intensity	Volume flux			Wilcoxon Rank sum	Moisture			Wilcoxon Rank sum	Pu-239 + 240			Wilcoxon Rank sum
	mm/min	— cm/event —				— m^3/m^3 —				— Bq/L —			
		X	SD	(N)		X	SD	(N)		X	SD	(N)	
Pit 2, 100 yr	1.28	0.33	0.1	(8)	$Z = -2.2$; $P > 0.02$	0.17	0.09	(21)	$Z = -3.4$; $P > 0.006$	2.25	3.6	(8)	$Z = -0.1$; $P > 0.87$
	2.03	0.68	0.3	(12)		0.27	0.07	(22)		0.85	1.5	(12)	
Pit 2, 50 yr	1.14	0.59	0.2	(13)	$Z = -0.9$; $P > 0.35$	0.22	0.08	(21)	$Z = -2.3$; $P > 0.01$	1.59	3.9	(13)	$Z = -0.7$; $P > 0.45$
	1.79	0.50	0.3	(13)		0.27	0.07	(22)		1.05	2.2	(13)	
Pit 3, 100 yr	1.28	0.48	0.3	(34)	$Z = -0.5$; $P > 0.62$	0.26	0.08	(46)	$Z = -1.5$; $P > 0.13$	0.61	0.8	(34)	$Z = -0.9$; $P > 0.34$
	2.03	0.51	0.3	(13)		0.23	0.09	(23)		0.79	1.5	(13)	

Table 7. Comparison between actinides activity, pH, specific conductance (SC), and alkalinity collected by ZTS and TS from the A horizon following a rain simulation of 100-yr event. These simulations were conducted in Julian Days 201, 202, and 203 in Pit 3.

Sampling device	N	Pu-239 + 240			Am-241			pH			SC			Alkalinity		
		X	m	SD	X	m	SD	X	m	SD	X	m	SD	X	m	SD
		— Bq/L —									— dsm^{-1} —			— mg/L —		
ZTS	15	1.7	0.78	1.87	0.3	0.10	0.43	6.84	6.84	0.20	0.21	0.22	0.03	50.2	48	10.3
TS	6	0.1	0.05	0.17	0.002	0.001	0.002	7.78	7.74	0.25	0.76	0.71	0.20	114	104	41.2
Wilcoxon Rank sum		$Z = -3.2$; $P > 0.001$			$Z = -3.2$; $P > 0.001$			$Z = -3.2$; $P > 0.001$			$Z = -3.2$; $P > 0.001$			$Z = -3.2$; $P > 0.001$		

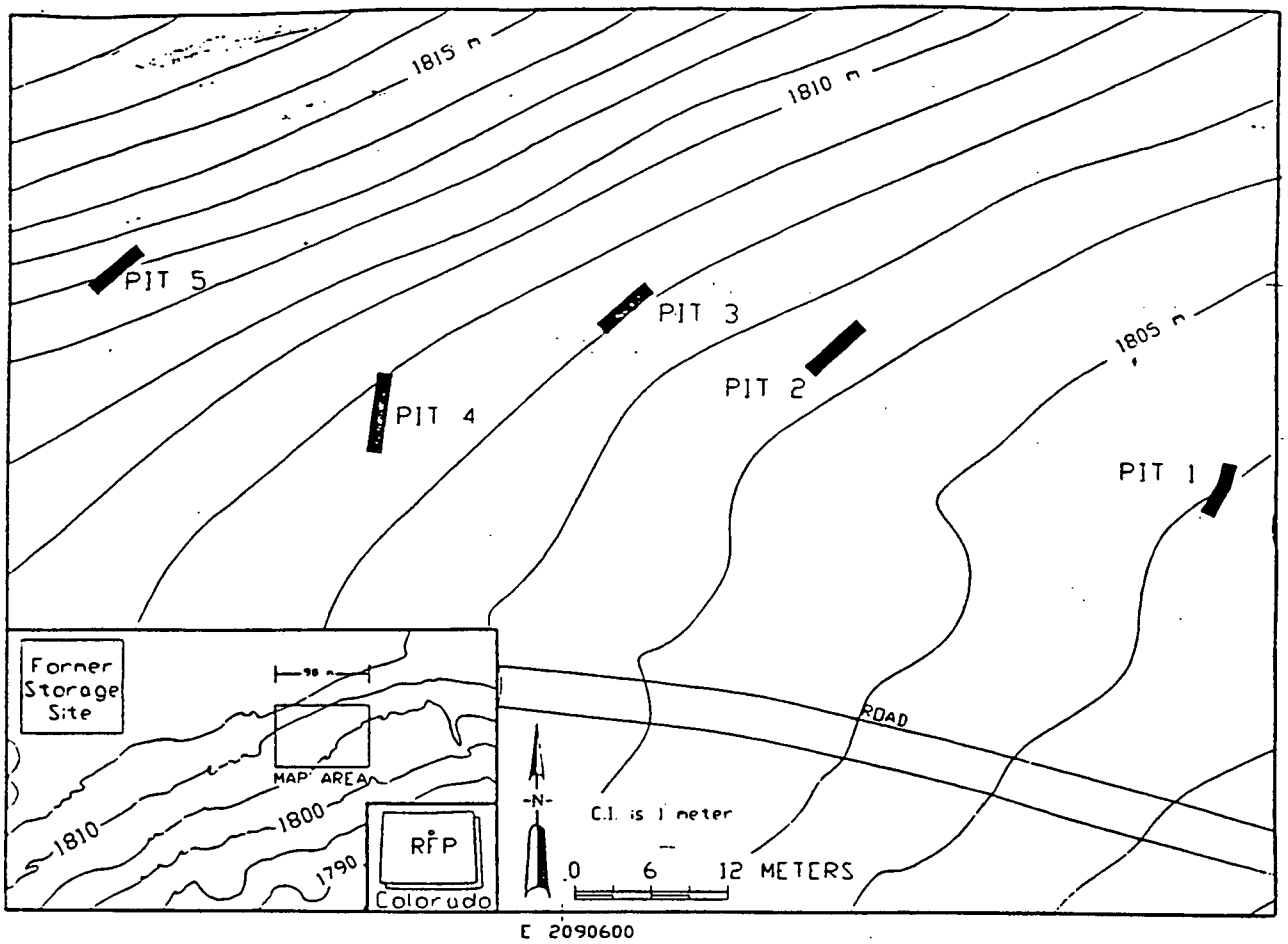

JOB NAME J&Q VOLUME 25 NUMBER 4 MONTH J-A COPY 6 of 15

AUTHOR	PG. #	FINAL WIDTH	FINAL HEIGHT		SCALE %	DENSITY	CHECKED BY
Litsor et al.	1	2col.		X LINE	75		
Q95-230	D B&W D COLOR	42	24 1/4	D HT D COMB			APPROVED FOR FILES SEND REVISE

PAGE NUMBER

watch fine lines

11

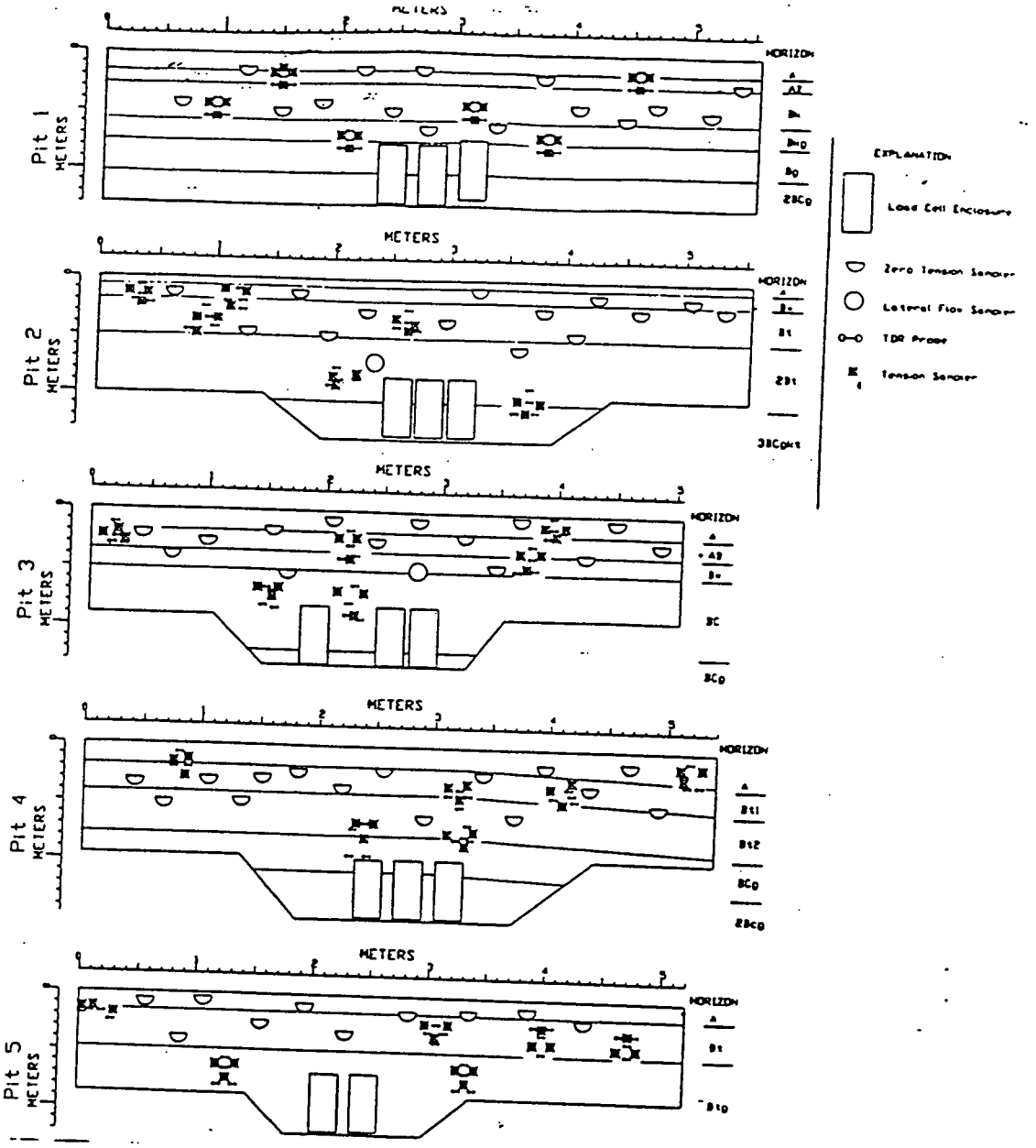

JOB NAME JEQ VOLUME 25 NUMBER 4 MONTH J-A

AUTHOR							
Litaor et al.	2	2col.		X LINE			CHECKED BY
Q95-230		42	48½		87		

(a) Pu-239+240 (Bq/Kg)

(b) Am-241 (Bq/Kg)

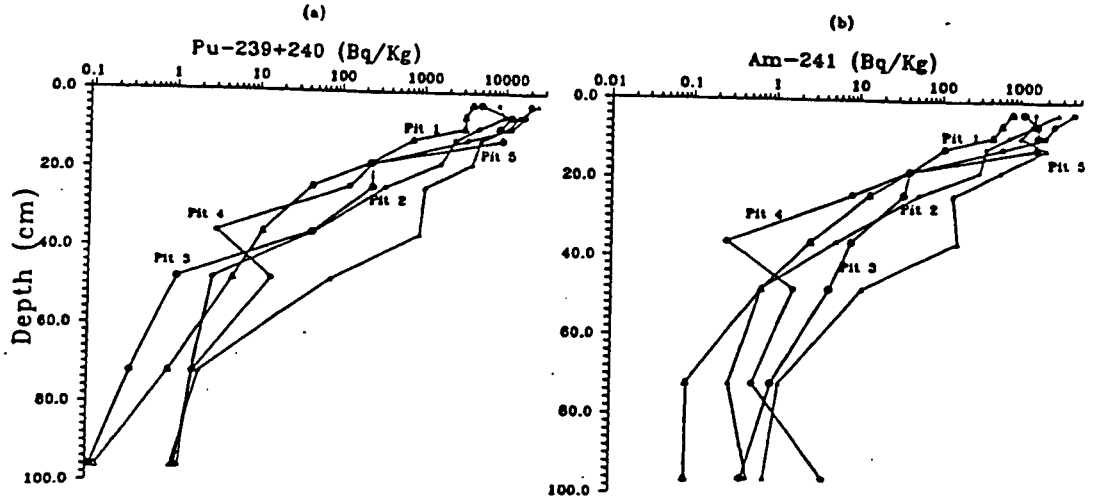

JOB NAME JEQ VOLUME 25 NUMBER 4 MONTH J-A

12

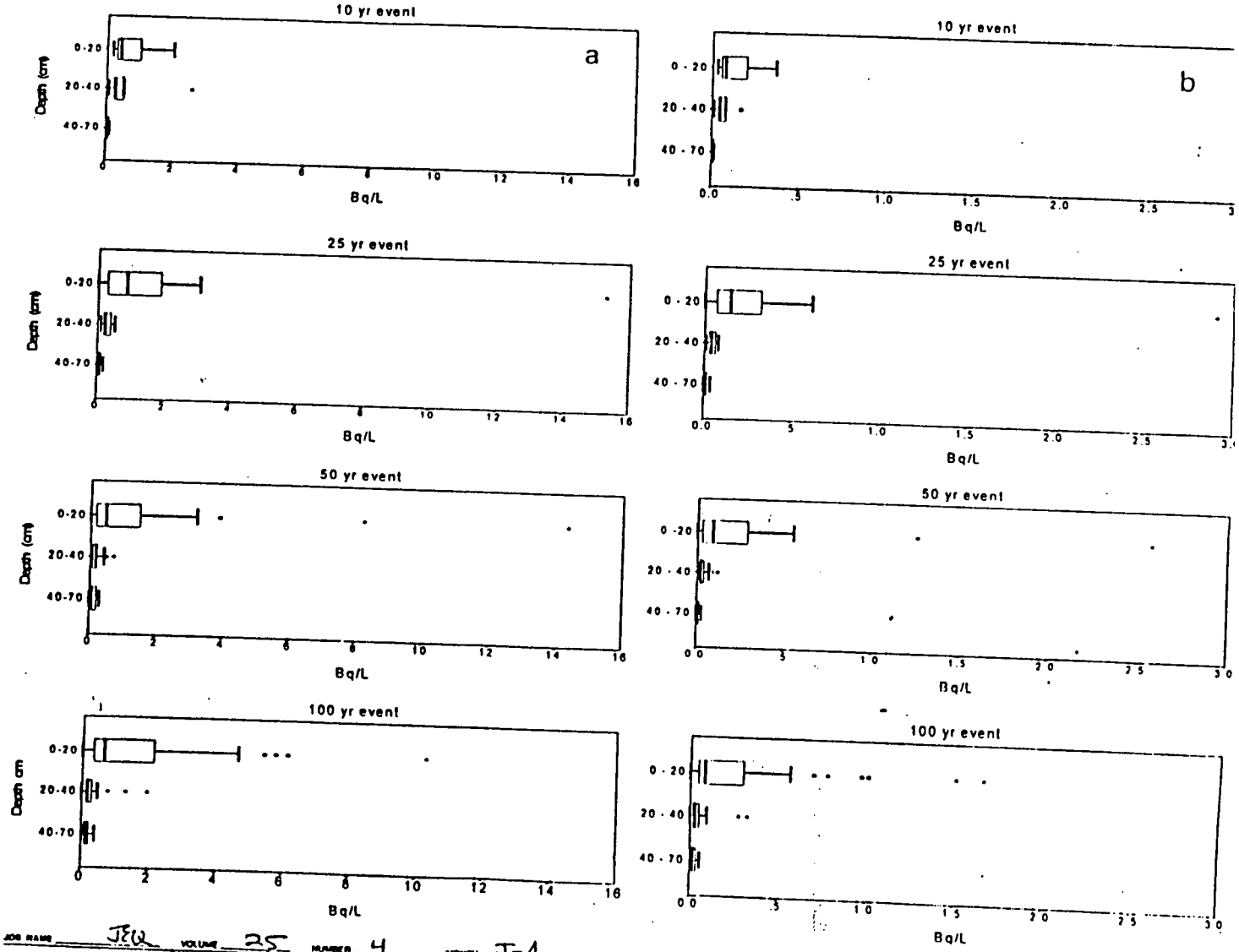

JEQ VOLUME 25 NUMBER 4 MONTH J-A

Litaor et al.

Julian Day 182, 25 Year Simulation (0.99 mm/min)

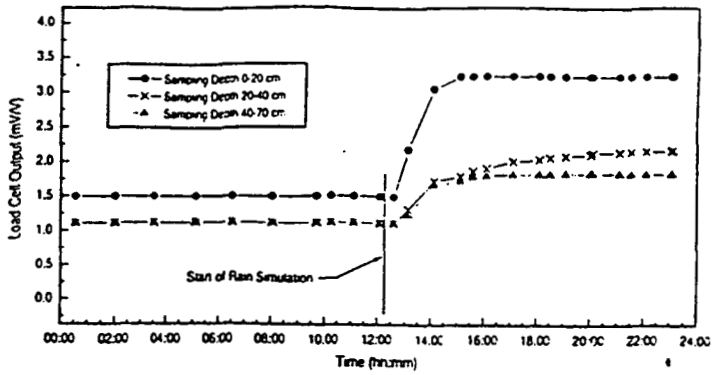

Julian Day 183, 50 Year Simulation, (1.14 mm/min)

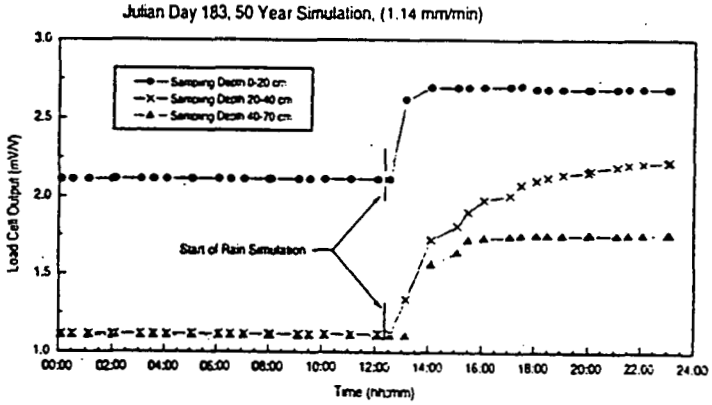

Julian Day 187, 100 Year Simulation, (1.28 mm/min)

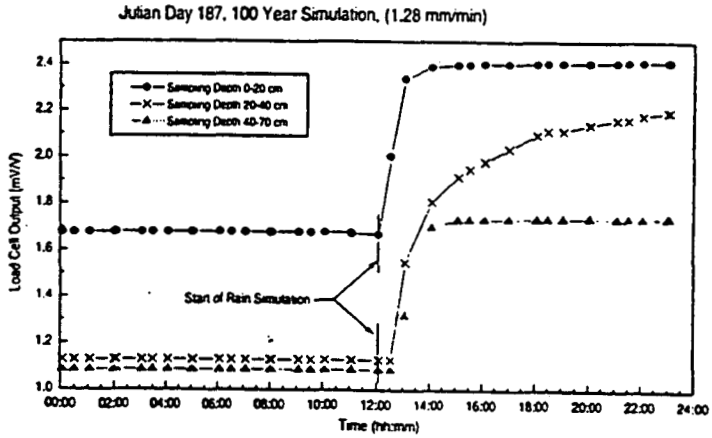

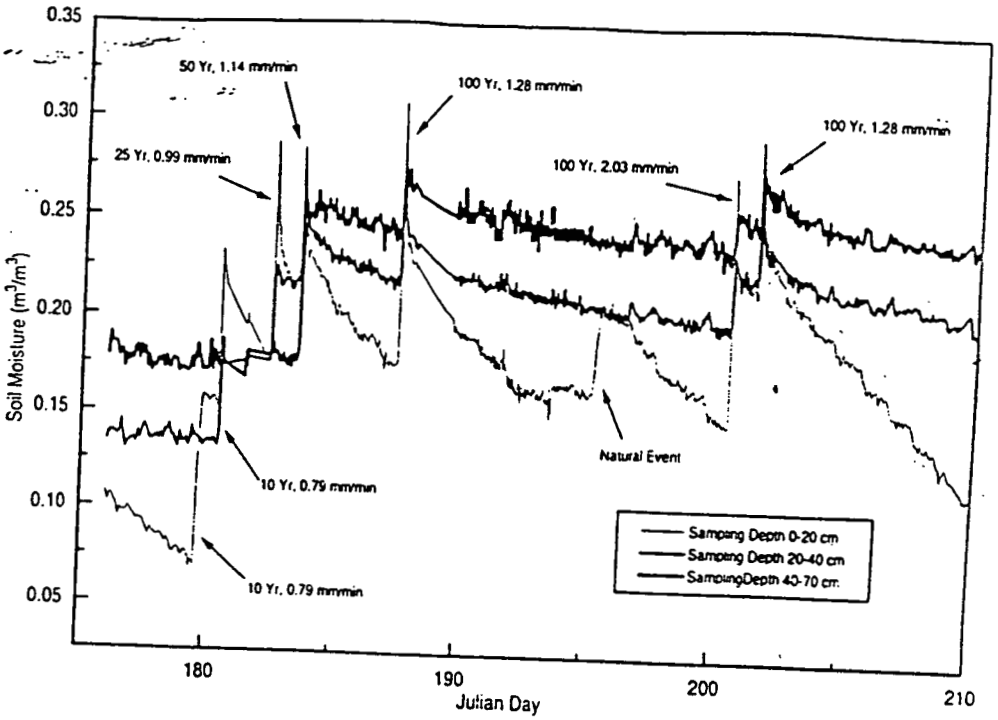

Figure 6

JEG 25 4 J-A

Litaor et al. 6 2col. 70

Q95-230 38 $26\frac{3}{4}$

SEP 2002
RECEIVED
RECORDS CENTER

15/15